Highly Selective Electroreduction N_2 and CO_2 to Urea over Artificial Frustrated Lewis Pairs

Menglei Yuan [1,2], Junwu Chen [1,2], Yong Xu [3], Rongji Liu [4], Tongkun Zhao [1,2], Jingxian Zhang [1,2], Zhongyu Ren [1,2], Zhanjun Liu [5], Carsten Streb [4], Hongyan He [1,2], Chao Yang [1,2,3], Suojiang Zhang [1,2], Guangjin Zhang [1,2,3*]

[1] CAS Key Laboratory of Green Process Engineering, State Key Laboratory of Multiphase Complex Systems, Institute of Process Engineering, Chinese Academy of Sciences, Beijing, 100190, China

[2] School of Chemical Engineering, Center of Materials Science and Optoeletronics Engineering, University of Chinese Academy of Sciences, Beijing, 100049, China

[3] Chemistry and Chemical Engineering Guangdong Laboratory, Shantou, 515031, China

[4] Institute of Inorganic Chemistry, Ulm University, Ulm, 89081, Germany

[5] State Key Laboratory of Coal Conversion, CAS Key Laboratory of Carbon Materials, Institute of Coal Chemistry, Chinese Academy of Sciences, Taiyuan, 030001, China

[*] Correpondence: zhanggj@ipe.ac.cn

Experimental Section

Materials

Nickle sulfate hexahydrate [$Ni(SO_4)_2 \cdot 6H_2O$, 99.99%], $NaBH_4$ [99.99%], phosphoric acid [H_3PO_4, ≥ 85%], sulfuric acid [H_2SO_4, ≥ 85%], iron chloride [$FeCl_3$, 99.9%], diacetylmonoxime [$C_4H_7NO_2$, AR], thiosemicarbazide [CH_5N_3S, 99%], ethanol [C_2H_6O, ≥99.8%] and potassium bicarbonate [$KHCO_3$, ≥ 99.99%] were purchased from Sigma-Aldrich Chemical Reagent Co., Ltd. Water (DI) were purified by Millipore system was utilized without further purification.

Preparation of pristine $Ni_3(BO_3)_2$

3 mmol $Ni(SO_4)_2 \cdot 6H_2O$ was dissolved in 285 mL of water. Then, 15 mL $NaBH_4$ solution (0.5 M) was added under ultrasonic conditions. After 1h reaction and 2h aging, the solids were collected by centrifugation and washed several times by water and ethanol. The final product was stored for further use after drying at room temperature.

Preparation of $Ni_3(BO_3)_2$-150 and $Ni_3(BO_3)_2$-250 catalysts

The pristine $Ni_3(BO_3)_2$ nanocrystals were annealed at 150°C and 250°C for 2h to obtain $Ni_3(BO_3)_2$-150 and $Ni_3(BO_3)_2$-250 catalysts.

Preparation of $Ni_3(BO_3)_2$-350, $Ni_3(BO_3)_2$-450 and $Ni_3(BO_3)_2$-150-4h catalysts

The pristine $Ni_3(BO_3)_2$ nanocrystals were annealed at 350°C and 450°C for 2h to obtain $Ni_3(BO_3)_2$-350 and $Ni_3(BO_3)_2$-450 catalysts. The pristine $Ni_3(BO_3)_2$ nanocrystals were annealed at 150°C for 4h to obtain $Ni_3(BO_3)_2$-150-4h catalysts.

Characterization

X-ray diffraction (XRD, X'PERT PRO MPD diffractometer, Cu Kα radiation,

λ=0.15418 nm, scanned range of 2-90°) was used to identify the crystal structure of all prepared catalysts. Scanning electron microscopy (SEM, JSM-7800F Prime) and transmission electron microscopy (TEM, JEM-2100F) were utilized to investigate the morphology of all samples. The Raman measurements were carried out on a Renishaw Raman Test system (λ=532 nm). Nitrogen and carbon dioxide temperature programmed desorption (TPD) were recorded on the AutoChem II2920. X-ray photoelectron spectroscopy (XPS) data were collected by using Krato, AXIS-HS monochromatized Al Kα cathode source of 75-150 W under ultrahigh vacuum. Fourier Transform Infrared Spectrometer (FTIR) and the spin state of the catalysts were tested on NICOLET Is 50 (Thermo) and MPMS-3 (Quantum Design), respectively. H NMR spectra were collected on a superconducting-magnet NMR spectrometer (Bruker AVANCE III HD 700 MHz).

Electrochemical measurements

All electrochemical characterizations were performed using a CHI 660E workstation coupled with a three-electrode system in a two-compartment cell separated by Nafion 211 membrane. And the Nafion membrane was treated by boiling in ultrapure water for 1 h and heating in H_2O_2 (5%) aqueous solution at 80℃ for another 1 h, respectively. Carbon cloth utilized in this work was purchased from CeTech (W1S1009 type) and treated with the mixture of H_2SO_4:H_2O_2 (1:3 vol.) for 12 h to remove surface impurities. To avoid contamination with nitrogen-containing species in air, electrodes were used either immediately after preparation or kept in vacuum before being used in electrochemical experiments. The prepared catalyst loaded on a piece of pretreated

carbon cloth (1×3 cm^2) was used as the working electrode, a graphite rod and Ag/AgCl (saturated KCl electrolyte) were employed as counter electrode and reference electrode, respectively. Potential without iR-compensated were converted to RHE scale via the following equation: E (vs. RHE) = E (vs. Ag/AgCl) + 0.0591 × pH + 0.197 (pH = 6.8 in CO_2-saturated electrolyte and N_2 + CO_2-saturated electrolyte in 0.1 M $KHCO_3$; pH = 8.3 for N_2-saturated electrolyte in 0.1 M $KHCO_3$). The catalyst ink for working electrode was prepared by dispersing 3.59 mg of catalyst in a mixed solution of 30 μL Nafion (0.5 wt%), 500 μL ethanol and 470 μL water followed by sonication for 30 minutes. Mass loading of 0.3 mg cm^{-2} was used for electrochemical study. All experiments were carried out at room temperature (25°C). To remove the impurities in the inlet gas, such as NO_X, the prepurification of high-purity N_2 (purity 99.999%) and CO_2 (purity 99.99%) by passing through a saturator filled with 0.05 M NaOH and a saturator filled with 0.05 M H_2SO_4 solution to remove any possible contaminants. Before carrying out all the electrochemical characterizations, the 0.1 M $KHCO_3$ electrolyte solution was purged with CO_2 + N_2 for 30 minutes. Cyclic voltammetry (CV) test was carried out on at a scan rate of 50 mV s^{-1} ranging from 0-0.2 V (vs. RHE). Linear sweep voltammetry (LSV) was also conducted at a scan rate of 5 mV s^{-1}. Chronoamperometric test were then conducted at different potentials and CO_2 + N_2 was continuously fed into the cathodic cell during the experiments. The recycle test was to perform five consecutive cycles of chronoamperometric runs without changing the electrolyte at -0.5 V vs. RHE.

Determination of urea concentration by diacetyl monoxime method

The urea concentration was determined by diacetyl monoxime method [*Clin Chim Acta.,* **1980,** *107,* 3-9]. 5g of diacetylmonoxime (DAMO) and 100 mg of thiosemicarbazide (TSC) were dissolved in distilled water and diluted to 1000 mL, denoted as DAMO-TSC solution. Then, 100 mL concentrated phosphoric acid was mixed with 300 mL of concentration sulfuric acid and 600 mL distilled water, then 100 mg $FeCl_3$ was dissolved in the above solution, denoted as acid-ferric solution. Typically, 1 mL of the sample solution was removed from the cathodic chamber. Afterwards, 1 mL of DAMO-TSC solution and 2 mL of acid-ferric solution were added into 1 ml of sample solution. Next, the mixed solution was heated to 100 ℃ and maintained at this temperature for 15 min. When the solution cooled to 25 ℃, the UV-Vis absorption spectrum was collected at a wave-length of 525 nm. The concentration-absorbance curve was calibrated using standard urea solution for a series of concentrations. The fitting curve shows good linear relation of absorbance value with urea concentration by three times independent calibration tests.

Calculation of Faradaic efficiency (FE) and urea formation rate

The FE for urea electrosynthesis was defined as the amount of electric charge used for producing urea divided the total charge passed through the electrodes during the electrolysis. Assuming six electrons were needed to produce one urea molecule, the FE was calculated according to the following equation:

$$FE = 6 \times F \times C_{urea} \times V / (60.06 \times Q)$$

The rate of formation of urea was calculated using the following equation:

$$\text{urea yield rate} = C_{urea} \times V / (m_{cat} \times t \times 60.06)$$

Where F is Faraday constant (96485 C mol^{-1}), C_{urea} is the measured mass concentration of urea; V is the volume of the cathodic reaction electrolyte; Q is the quantity of applied charge/electricity; t is the time for which the potential was applied; m is the mass of catalyst loaded at the carbon cloth.

Determination of NH_3 concentration by indophenol blue method

When tested in 0.1 M $KHCO_3$, the produced NH_3 was spectrophotometrically determined by the indophenol blue method [*Nat Mater.* **2013,** *12*, 836-841]. Typically, 2 mL of the sample solution was removed from the cathodic chamber. Afterwards, 2 mL of 1.0 M NaOH solution containing 5 wt% salicylic acid and 5 wt% sodium citrate was added, followed by 1 mL NaClO solution (0.05 M) and 0.2 mL of an aqueous solution of sodium nitroferricyanide (1 wt%) were added. After standing at room temperature for 2 hours, the UV-Vis absorption spectrum was collected at a wave-length of 655 nm. The concentration-absorbance curve was calibrated using standard NH_4Cl solution for a series of concentrations. The fitting curve shows good linear relation of absorbance value with NH_4Cl concentration by three times independent calibration tests.

Calculation of Faradaic efficiency (FE) and NH_3 formation rate

The FE for NRR was defined as the amount of electric charge used for producing NH_3 divided the total charge passed through the electrodes during the electrolysis. Assuming three electrons were needed to produce one NH_3 molecule, the FE was calculated according to the following equation:

$$FE = 3 \times 0.318 \times F \times C_{NH4Cl} \times V / (17 \times Q)$$

The rate of formation of NH3 was calculated using the following equation:

$$NH_3 \text{ yield rate} = 0.318 \times C_{NH4Cl} \times V / (m_{cat} \times t \times 53.5)$$

Where F is Faraday constant (96485 C mol^{-1}), C_{NH4Cl} is the measured mass concentration of NH_4Cl; V is the volume of the cathodic reaction electrolyte; Q is the quantity of applied charge/electricity; t is the time for which the potential was applied; m_{cat} is the mass of catalyst loaded at the carbon cloth.

DFT calculations

Spin-polarized density functional theory (DFT) calculations were conducted using the Vienna ab initio simulation package (VASP) [*Matter Mater. Phys.,* **1996**, *54,* 11169–11186; *Comput. Mater. Sci.,* **1996**, *6,* 15–50]. The projector augmented wave (PAW) method was used to describe electron-ion interactions. A generalized gradient approximation (GGA) to the exchange–correlation functional of Perdew–Burke–Ernzernhof (PBE) with DFT+U correction (U − J = 6.2 eV for Ni 3d) was applied [*Matter Mater. Phys.,* **1992**, *45,* 13244–13249; *Phys. Rev. Lett.,* **1996**, *77*, 3865−3868]. A Gaussian smearing of 0.05 eV was applied. The cutoff energy for plane-wave basis set was set as 520 eV, and the total energy convergence was set to be lower than 2×10^{-6} eV, with the force convergence set at 0.02 eV/Å for geometric optimizations. A Monkhorst-Pack k-points setting of 3 × 3 × 1 and 6 × 6 × 1 was used to sample the Brillouin zone for geometry optimizations and electronic structure computations, respectively. The DFT-D3 empirical correction method was employed to describe van der Waals interactions [*J. Chem. Phys.,* **2010,** *132,* 154104]. The free energy of the electrochemical steps of the reaction was calculated based on the computational hydrogen electrode (CHE) model. The free energies of species were calculated as G =

E_{DFT} + E_{ZPE} - TΔS, where E_{DFT} was obtained from DFT energy, $E_{ZPE,}$ and TΔS of adsorbed species were calculated by vibration analysis, whereas the thermodynamic corrections for gas molecules were from the standard database.

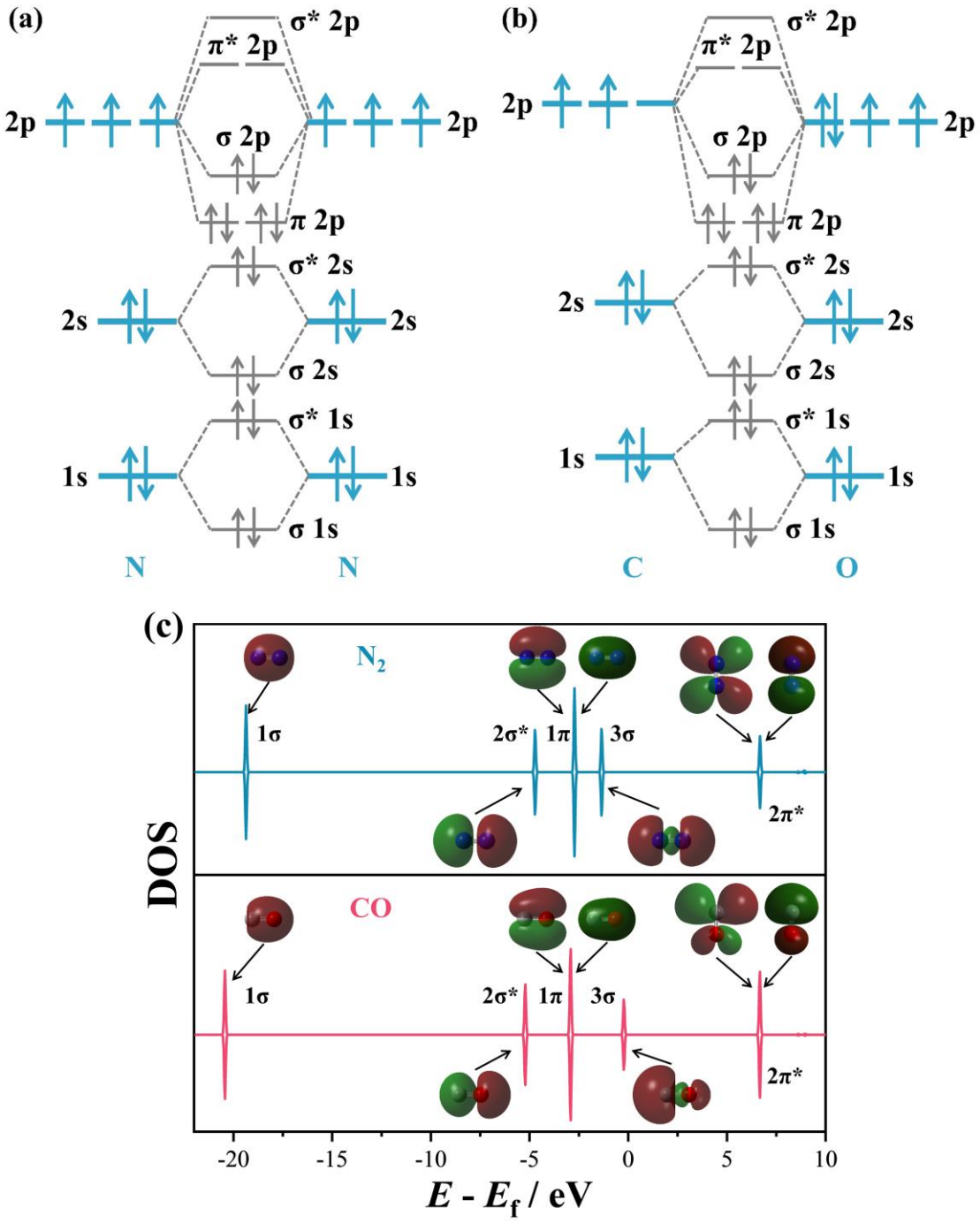

Figure S1. The molecular orbitals of (a) *N_2 and (b) *CO_2; (c) the calculated orbital energy levels of CO and N_2 by density of states (DOS).

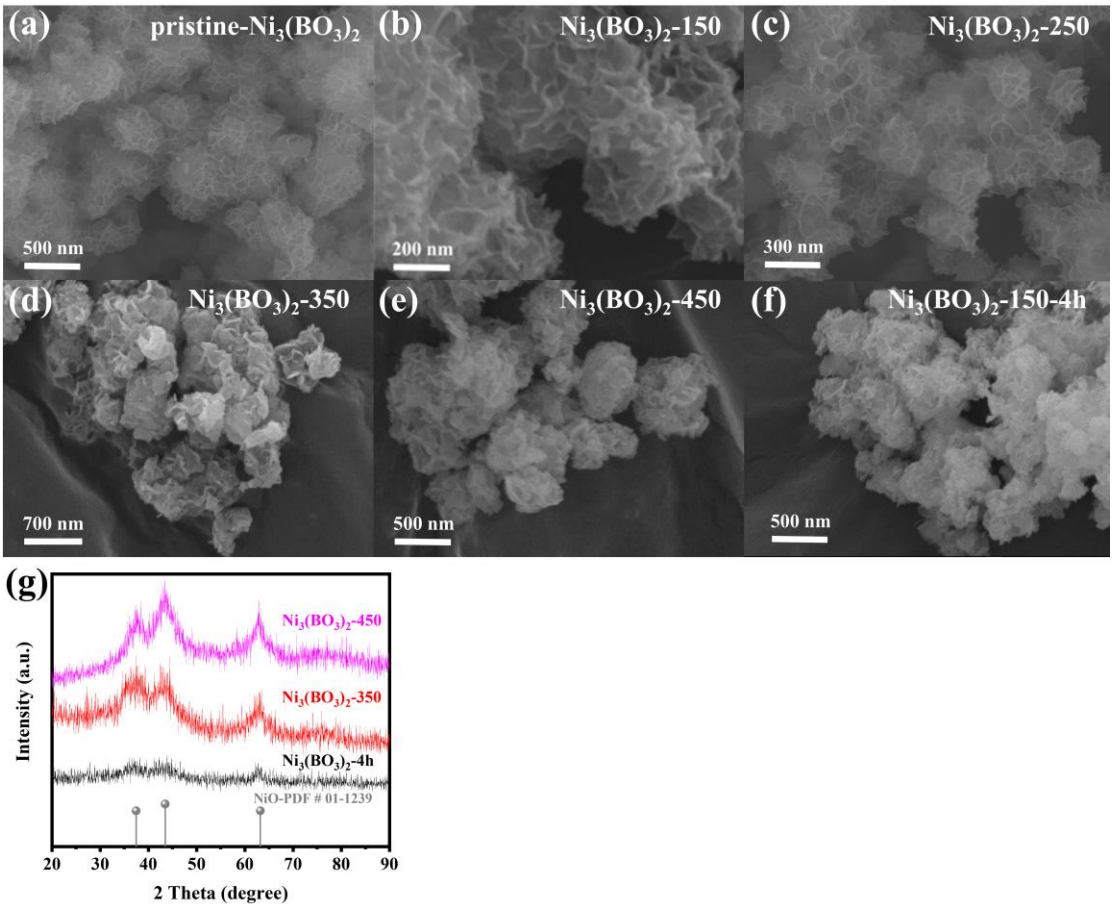

Figure S2. The SEM images of (a) pristine $Ni_3(BO_3)_2$; (b) $Ni_3(BO_3)_2$-150; (c) $Ni_3(BO_3)_2$-250; (d) $Ni_3(BO_3)_2$-350; (e) $Ni_3(BO_3)_2$-450; (f) $Ni_3(BO_3)_2$-150-4h; (g) the XRD patterns of $Ni_3(BO_3)_2$-350, $Ni_3(BO_3)_2$-450 and $Ni_3(BO_3)_2$-150-4h catalysts.

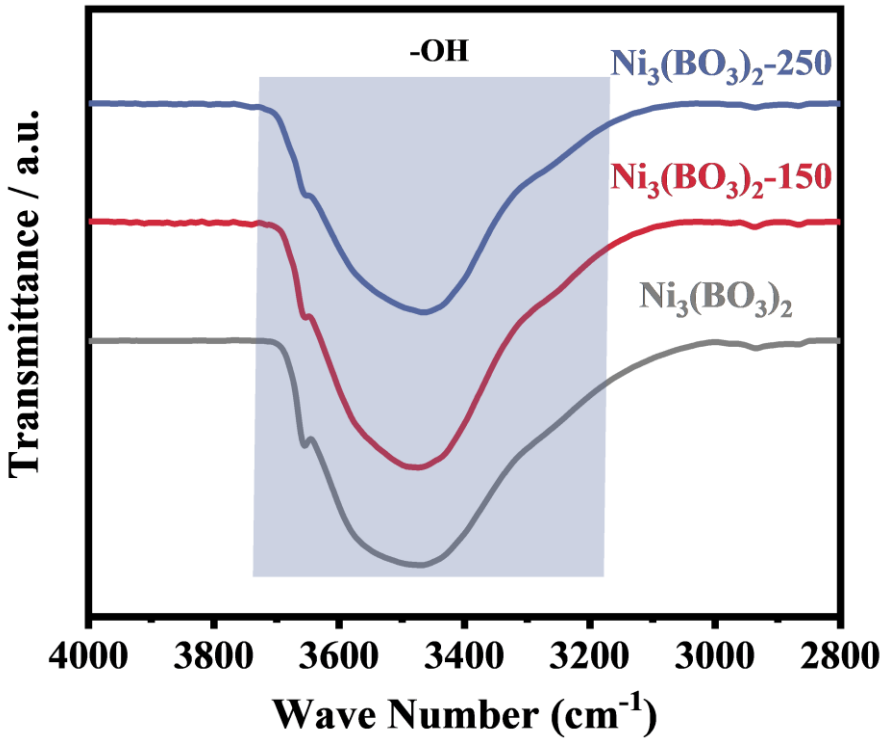

Figure S3. The FTIR spectrum of pristine $Ni_3(BO_3)_2$, $Ni_3(BO_3)_2$-150 and $Ni_3(BO_3)_2$-250 catalysts.

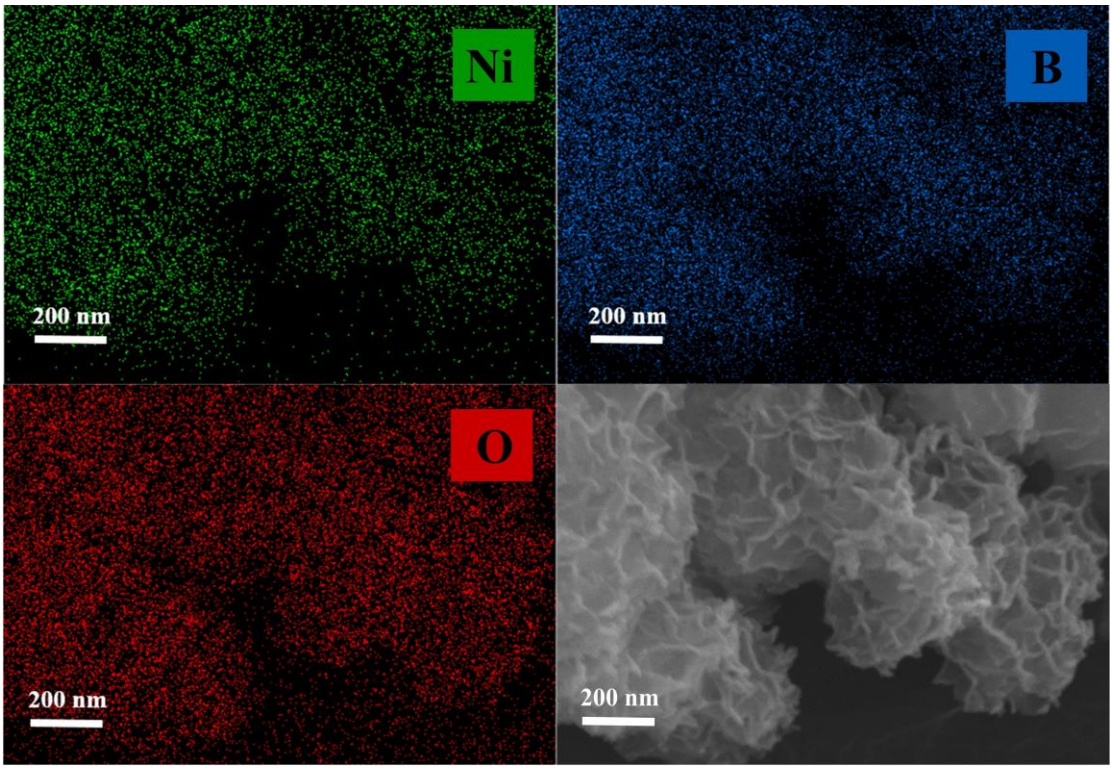

Figure S4. The EDX elemental mapping of the $Ni_3(BO_3)_2$-150 catalysts.

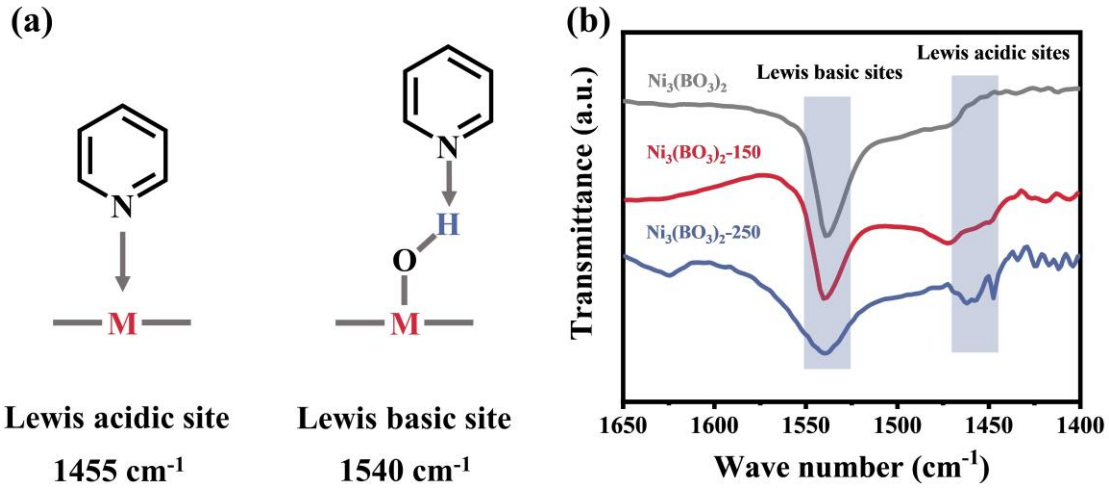

Figure S5. (a) The schematic illustration of pyridine chemisorption on Lewis acidic site and Lewis basic site; (b) pyridine adsorption infrared spectroscopy (Py-IR) of the pristine $Ni_3(BO_3)_2$, $Ni_3(BO_3)_2$-150 and $Ni_3(BO_3)_2$-250 catalysts.

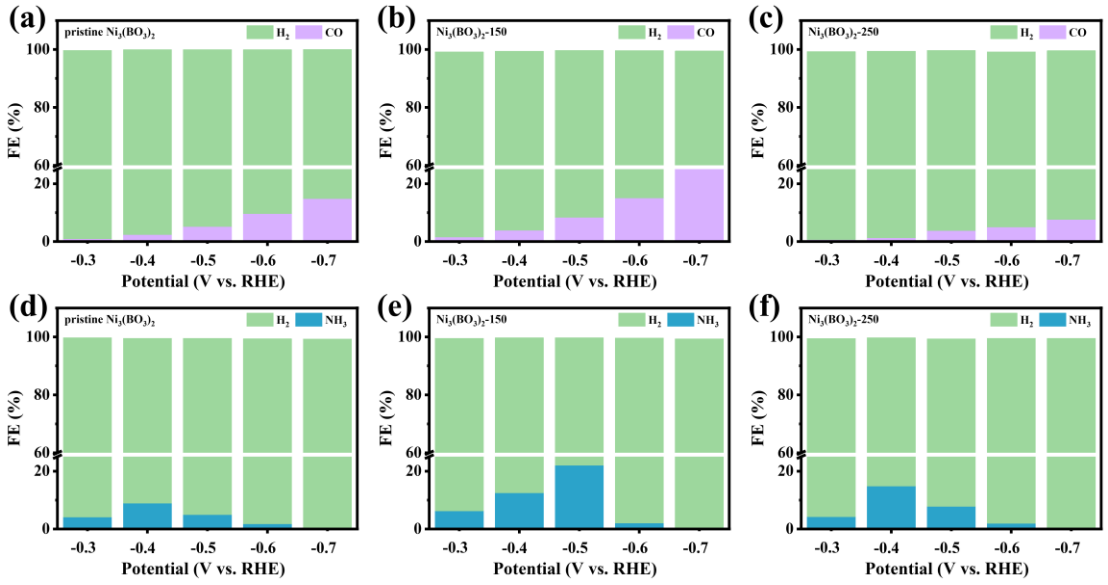

Figure S6. The product distribution of pristine $Ni_3(BO_3)_2$, $Ni_3(BO_3)_2$-150 and $Ni_3(BO_3)_2$-250 catalysts for (a-c) CO_2RR and (d-f) NRR.

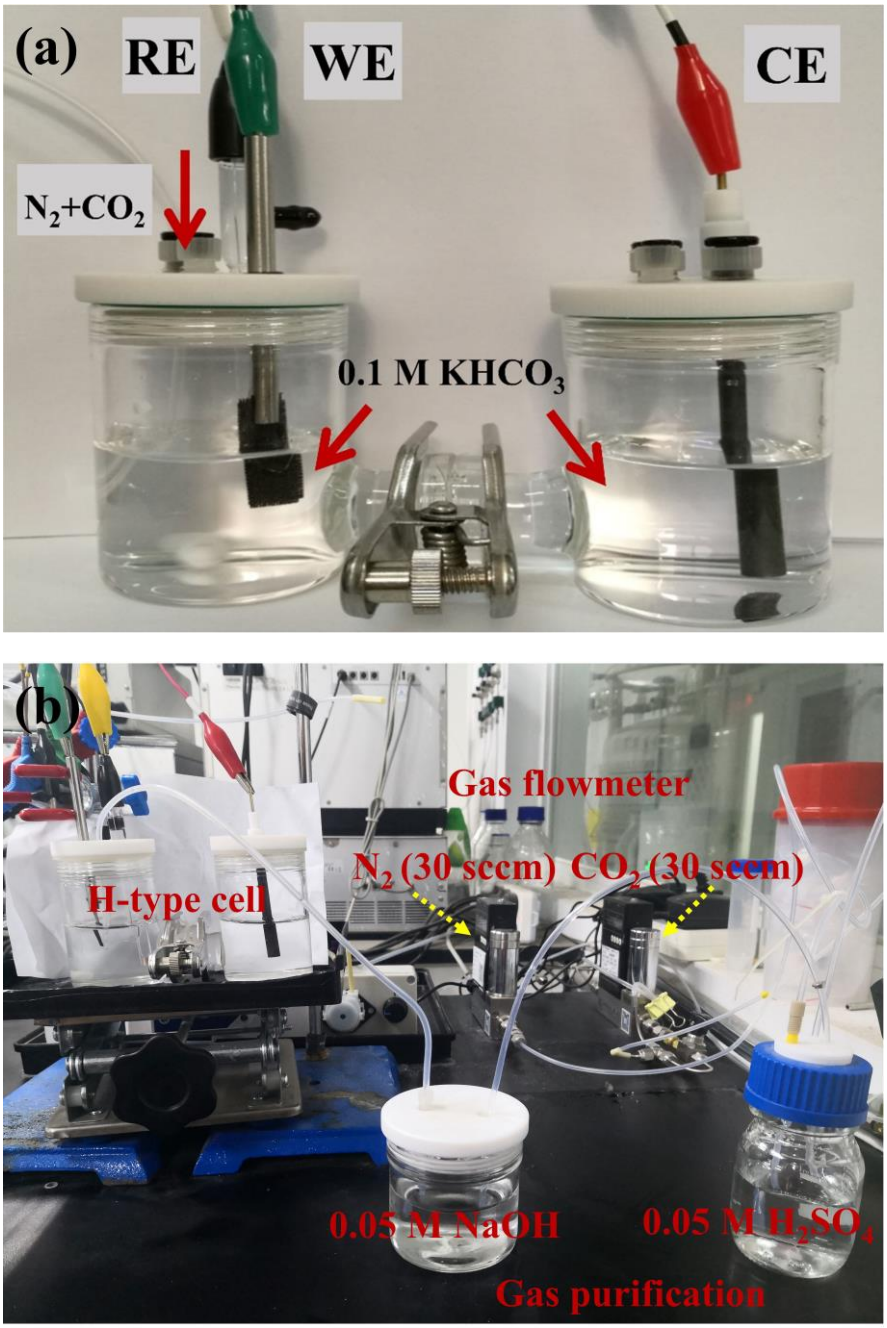

Flow rate: N_2 (30 sccm); CO_2 (30 sccm)
Purification time: 12 h
Purification agents: 0.05 M NaOH; 0.05 M H_2SO_4

Figure S7. (a) The optical photograph of the H-type cell for urea electrosynthesis testing; (b) the optical photograph of detailed experimental set-up for both N_2 and CO_2 gas purification.

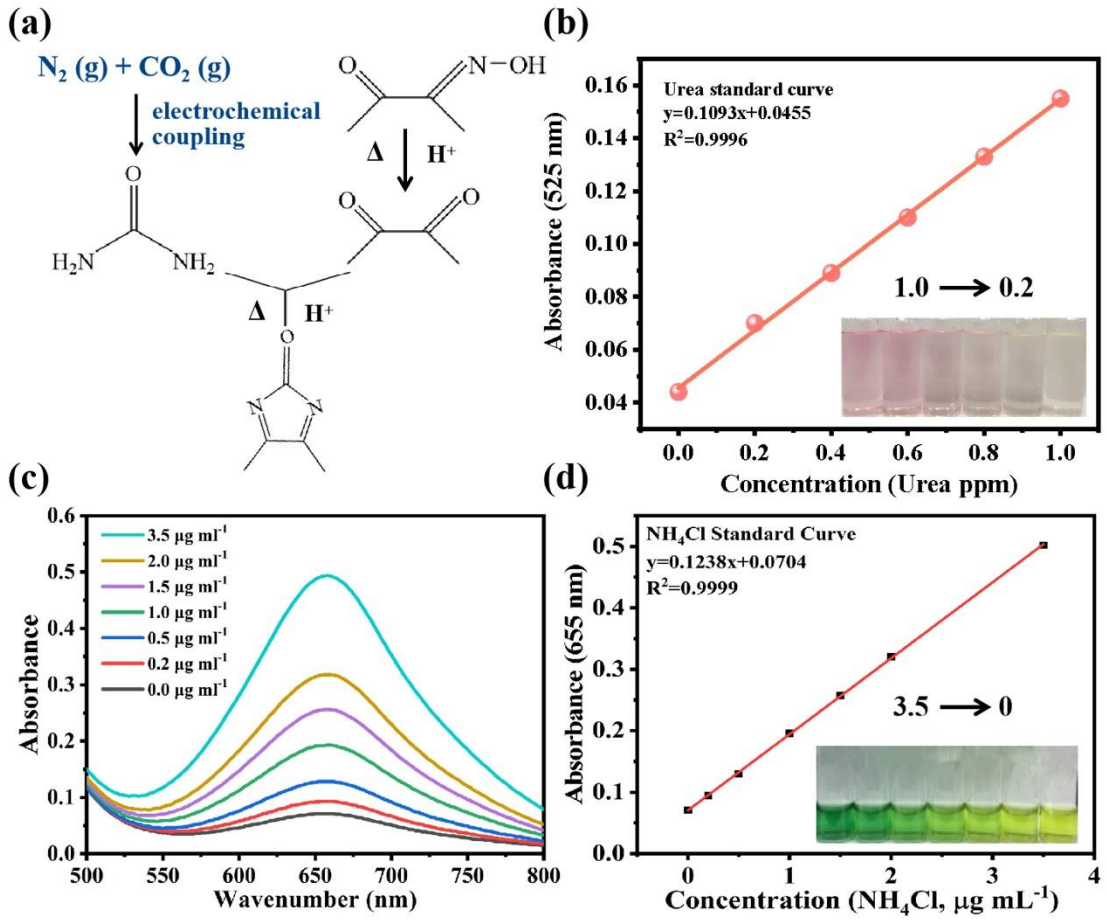

Figure S8. (a) Experimental scheme for the electrochemical synthesis of urea and subsequent determination of the urea concentration generated. Urea detection is based on the diacetyl monoxime method; (b) concentration-absorbance of urea solution with a series of standard concentration (0.2-1.0 μg mL^{-1}) in 0.1 M $KHCO_3$. The absorbance at 525 nm was measured by UV-vis spectrophotometer. The standard curve shown good linear relation of absorbance with urea concentration (y=0.1093x+0.0455, R^2=0.9996); (c) UV-vis curves and (d) concentration-absorbance of NH_4Cl solution with a series of standard concentration (0-3.5 μg mL^{-1}) in 0.1 M $KHCO_3$. The absorbance at 655 nm was measured by UV-vis spectrophotometer. The standard curve shown good linear relation of absorbance with NH_4Cl concentration (y=0.1238x+0.0704, R^2=0.9999).

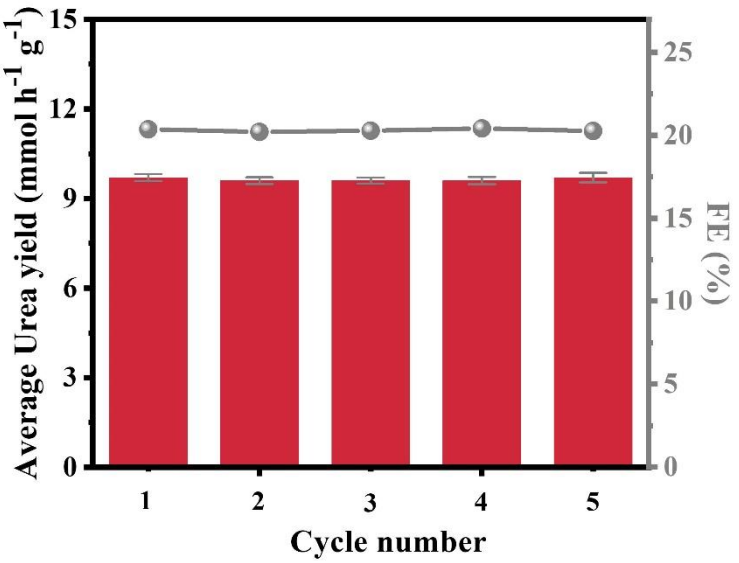

Figure S9. The Faradaic efficiency and urea production rate of $Ni_3(BO_3)_2$-150 catalyst at -0.5 V vs. RHE during recycling tests for five times.

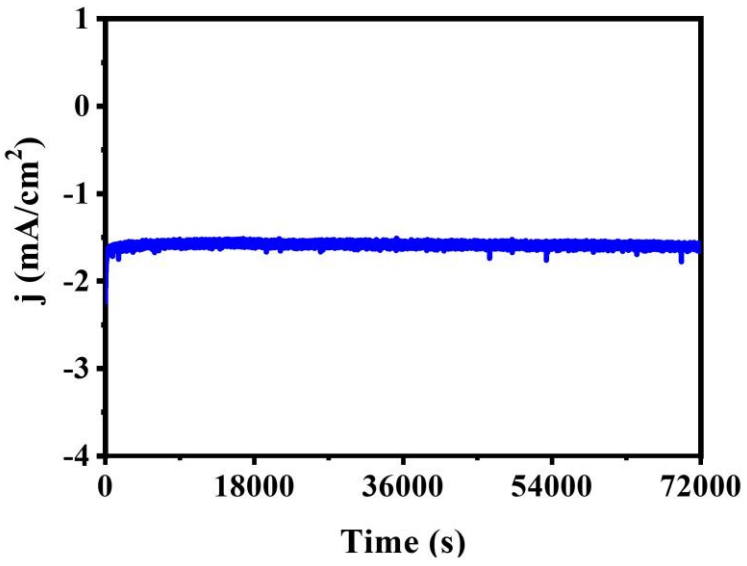

Figure S10. The chronamperometric curves of $Ni_3(BO_3)_2$-150 catalyst at -0.5 V vs. RHE for 20 h in N_2 + CO_2-saturated in 0.1 M $KHCO_3$ solution.

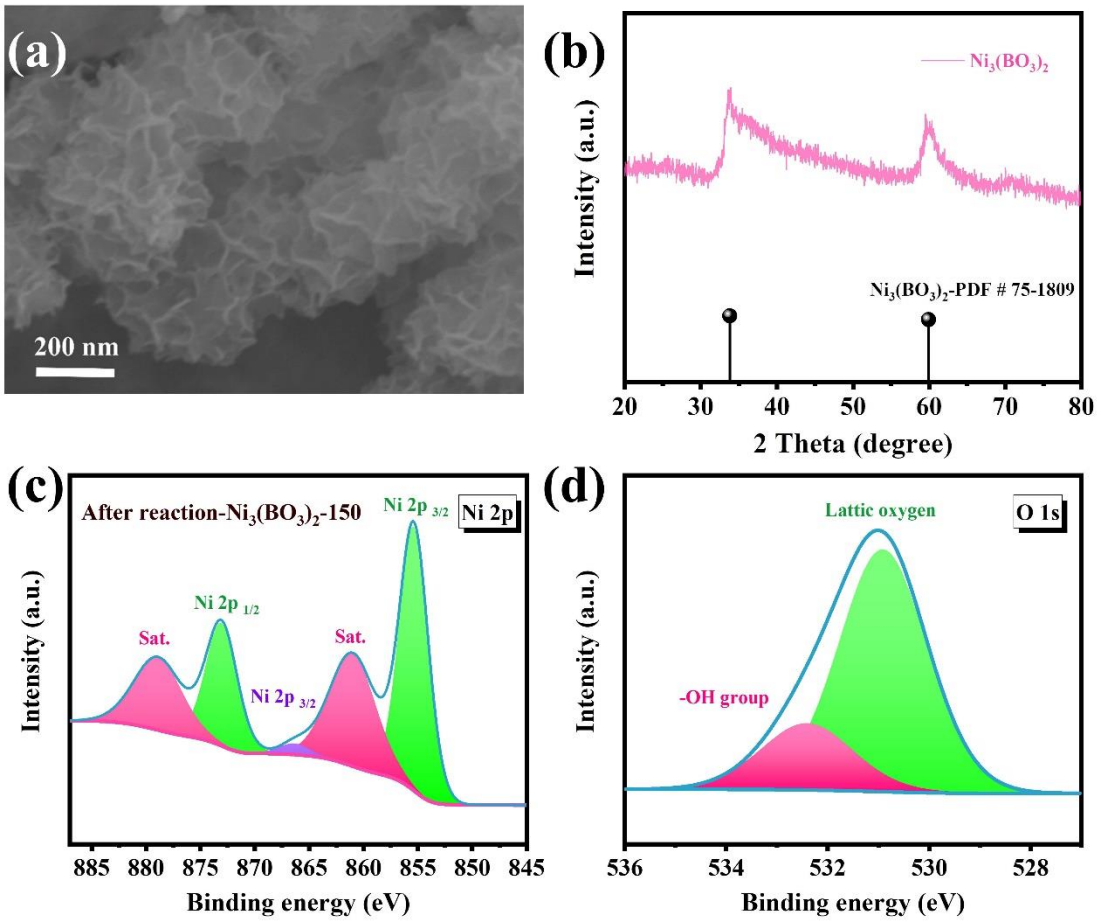

Figure S11. (a) SEM image; (b) XRD pattern; (c) high-resolution Ni 2p spectrum and (d) O 1s spectrum of $Ni_3(BO_3)_2$-150 catalyst after 20h electrolysis.

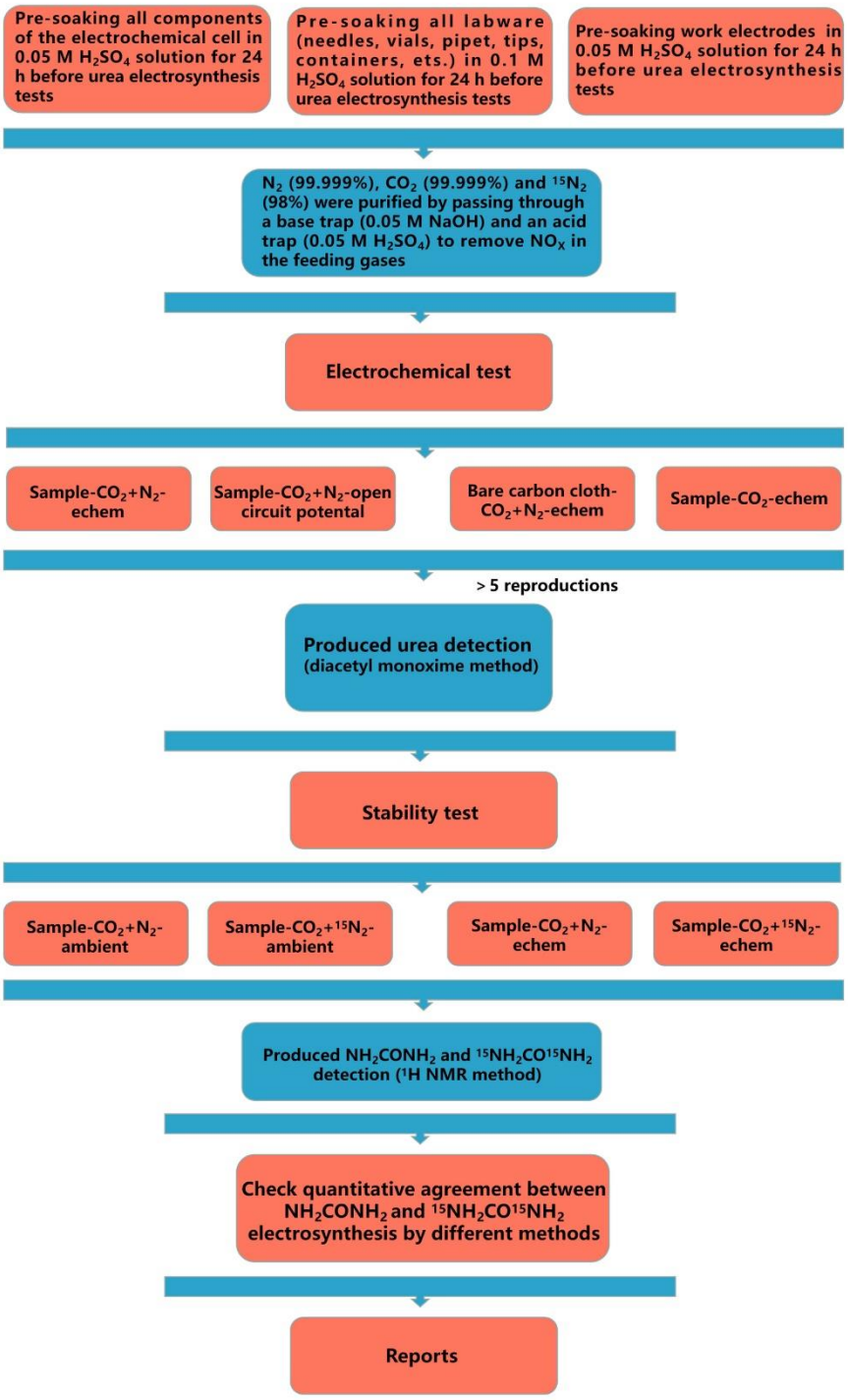

Scheme S1. The urea electrosynthesis experimental produces we utilized in this work.

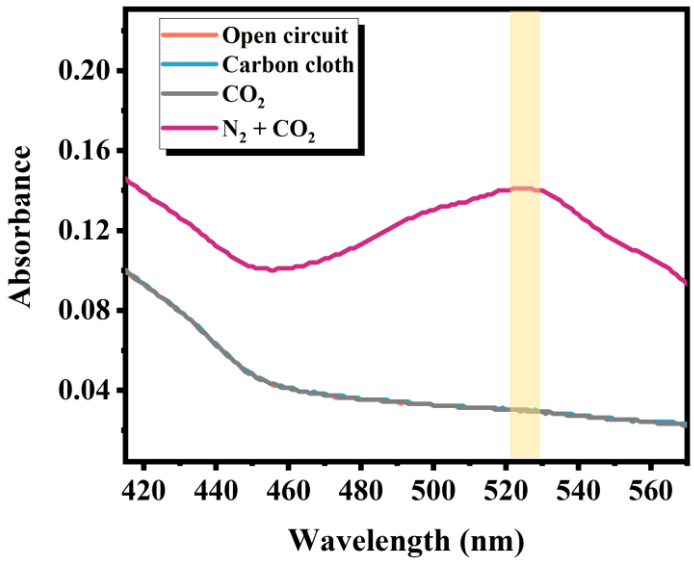

Figure S12. UV-vis spectra of the electrolyte stained with diacetyl monoxime indicator for the bare carbon cloth electrolysis 2h in N_2+CO_2-saturated solution, without and after 2h electrolysis at the potential of -0.5 V in N_2+CO_2-saturated solution, electrolysis 2h in CO_2-saturated solution.

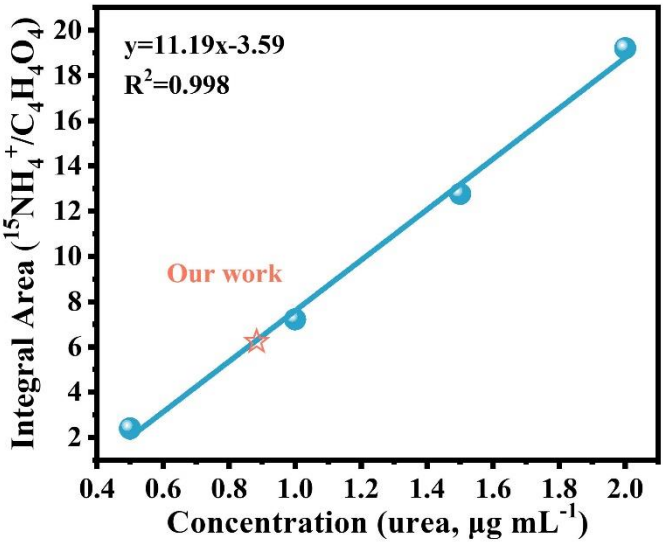

Figure S13. Integral area ($^{15}NH_2CO^{15}NH_2$ / $C_4H_4O_4$) - concentration linear relation calibrated using standard $^{15}NH_2CO^{15}NH_2$ solution.

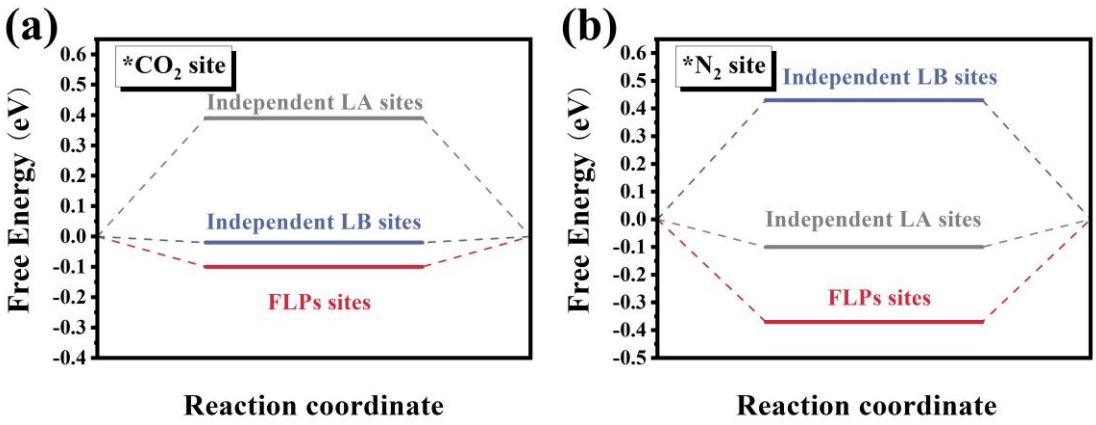

Figure S14. The chemisorption of (a) CO_2 and (b) N_2 on all possible active sites.

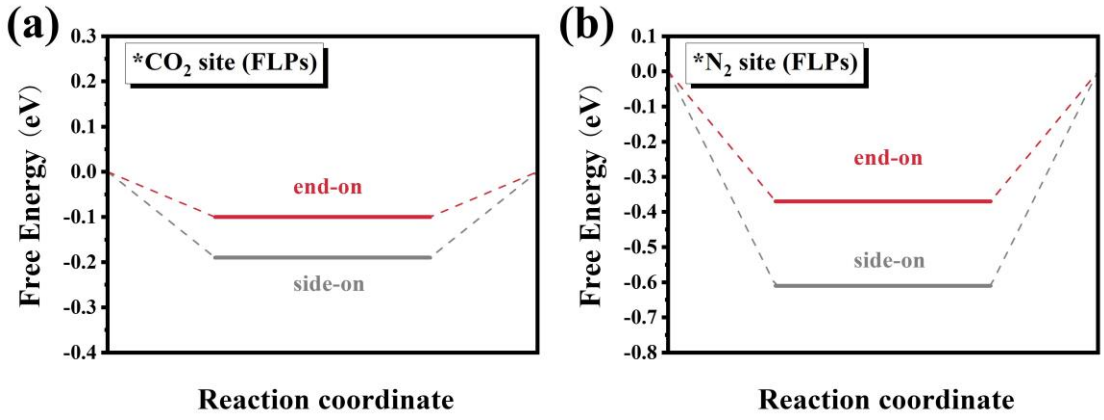

Figure S15. The chemisorption of (a) CO_2 and (b) N_2 on the FLPs sites via end-on and side-on configuration.

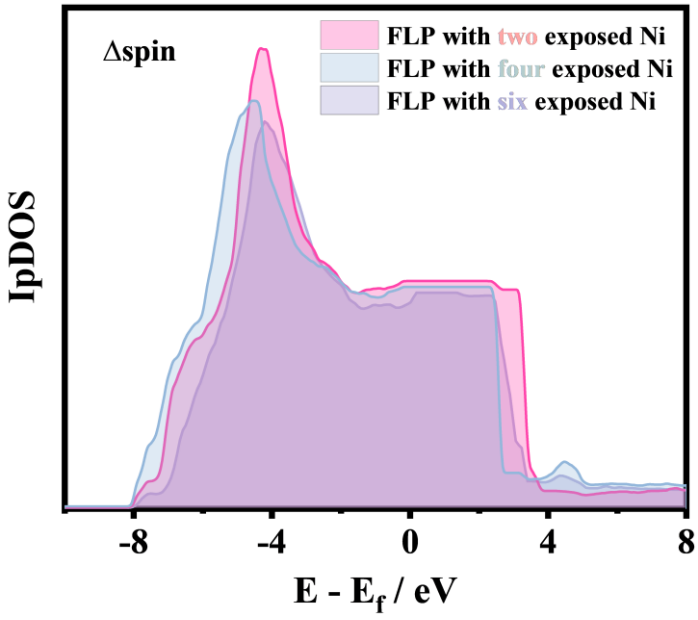

Figure S16. The net spin up ($\Delta_{spin\text{-}up}$) of artificial FLPs with different number of exposed Ni sites.

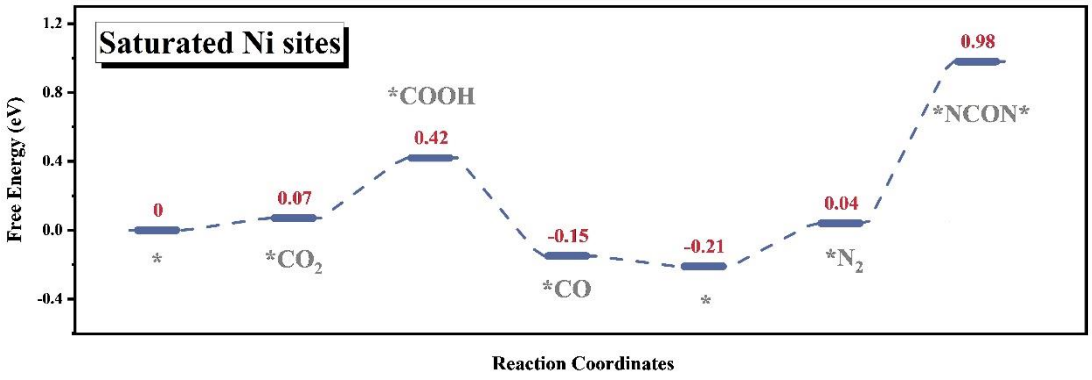

Figure S17. The free energy diagrams for the *NCON* formation on the saturated Ni sites (in bulk) of $Ni_3(BO_3)_2$-150 catalyst.

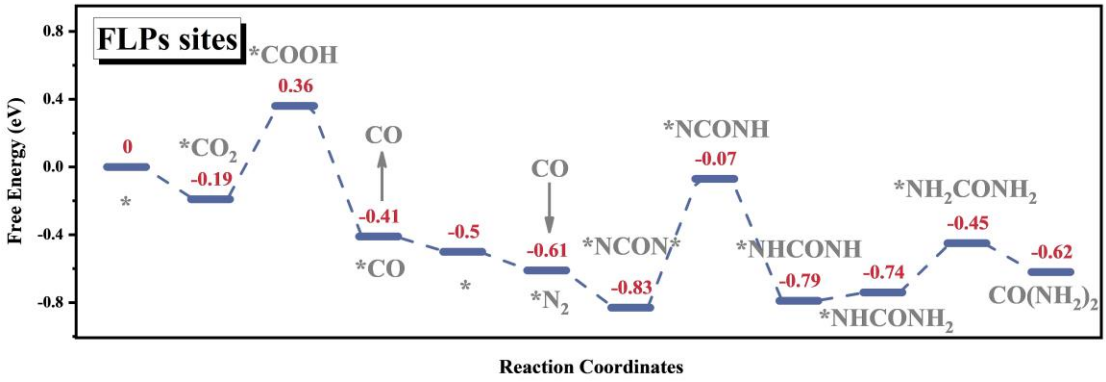

Figure S18. The free energy diagrams of electrocatalytic urea synthesis over artificial FLPs sites in $Ni_3(BO_3)_2$-150 catalyst.

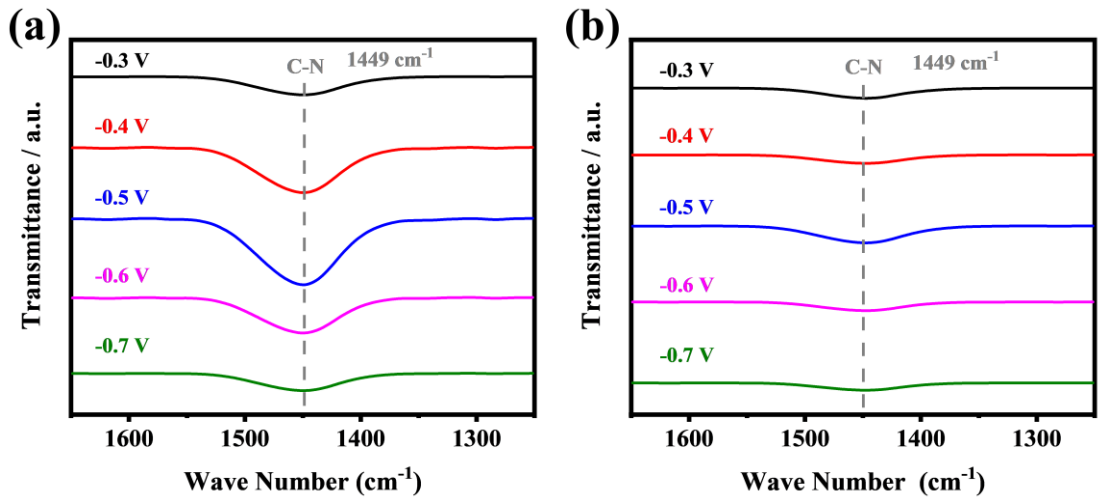

Figure S19. The *in situ* SR-FTIR spectroscopy of (a) $Ni_3(BO_3)_2$-150 catalyst and (b) pristine $Ni_3(BO_3)_2$ catalyst.

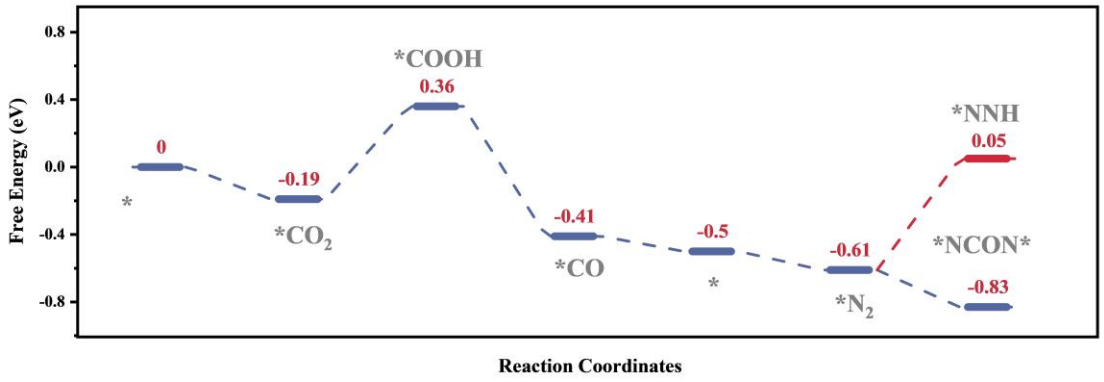

Figure S20. The free energy diagrams for N_2 adsorption and further activation on the $Ni_3(BO_3)_2$-150 catalyst.

Table S1. The ICP-OES results of all prepared catalysts

	Pristine $Ni_3(BO_3)_2$	$Ni_3(BO_3)_2$-150	$Ni_3(BO_3)_2$-250
ICP-OES (Ni, wt %)	11.368	11.366	11.366

Table S2. The Weiss constant θ and effective paramagnetic moment μ_{eff} of pristine $Ni_3(BO_3)_2$ and $Ni_3(BO_3)_2$-150 catalysts.

	Pristine $Ni_3(BO_3)_2$	$Ni_3(BO_3)_2$ -150
θ (K)	69.1	-2.8
μ_{eff} (μ_B)	3.3863	1.5707

Table S3. Concentration of potential NH_3, NOx and N_2O contaminants supplied in 12h experiments using different feed gas.

Gas	Flow rate (sccm)	Purging time (min)	Volume of gas used (mL)	NH_3* (ng mL^{-1})	NO_x* (ng mL^{-1})	N_2O (ppm)
Commercial $^{14}N_2$	30	720	21600	2.24#	10.89	0.05#
Purified $^{14}N_2$				2.24#	6.32#	0.05#
Commercial CO_2	30	720	21600	2.24#	12.33	0.05#
Purified CO_2				2.24#	6.32#	0.05#

*The concentrations of NOx and NH_3 were calculated based on 80 mL electrolyte.
#For the contaminants that were not detected, their corresponding concentration was assumed to be equal to the related limit of detection

Table S4. Comparison of the urea electrosynthesis activity of $Ni_3(BO_3)_2$-150 catalyst with previously reported urea electrosynthesis catalysts.

Catalysts	Electrolyte	Potential (V vs. RHE)	Faradaic efficiency	Urea yield rate	Reference
$Ni_3(BO_3)_2$-150	0.1 M $KHCO_3$	-0.5 V	20.36 %	9.70 mmol h^{-1} g^{-1}	This work
Pd_1Cu_1/TiO_2-400	0.1 M $KHCO_3$	-0.4 V	8.92 %	3.36 mmol h^{-1} g^{-1}	Nat Chem., 2020, 12, 717-724
Bi-$BiVO_4$ hybrids	0.1 M $KHCO_3$	-0.4 V	12.55 %	5.91 mmol h^{-1} g^{-1}	Angew Chem Int Ed., 2021, 60, 10910-10918
$BiFeO_3/BiVO_4$ hybrids	0.1 M $KHCO_3$	-0.4 V	17.18 %	4.94 mmol h^{-1} g^{-1}	Chem Sci., 2021, 12, 6048
Te-Pd nanocrystal	0.1 M $KHCO_3$ + 0.01 M KNO_2	-1.1 V	12.2 %	--	Nano Lett., 2020, 20, 8282-8289